Molecular Crystals and Liquid Crystals
Publication details, including instructions for authors and subscription information:
http://www.tandfonline.com/loi/gmcl16

Surface Excitons in Crystal Anthracene

G. C. Morris [a b] & M. G. Sceats [c]
[a] Department of Chemistry, University of Queensland, St. Lucia, 4067, Australia
[b] The Davy Faraday Laboratory, The Royal Institution, London
[c] Department of Chemistry, University of Queensland, St. Lucia, Australia
Version of record first published: 29 Aug 2007.

To cite this article: G. C. Morris & M. G. Sceats (1974): Surface Excitons in Crystal Anthracene, Molecular Crystals and Liquid Crystals, 25:3-4, 339-359

To link to this article: http://dx.doi.org/10.1080/15421407408082811

Mol. Cryst. Liq. Cryst., 1974, Vol. 25, pp. 339-359

Printed in Dordrecht, Holland

Surface Excitons in Crystal Anthracene

G. C. MORRIS

Department of Chemistry, University of Queensland, St. Lucia, 4067, Australia
and
The Davy Faraday Laboratory, The Royal Institution, London.

and

M. G. SCEATS

Department of Chemistry, University of Queensland, St. Lucia, 4067, Australia

(Received August 8, 1973)

Normal incidence reflection spectra from artificially surface roughened anthracene crystals probed on the (ab) face provide evidence for a roughness induced surface molecular exciton. The frequency at which the resonance associated with that surface exciton appears is predicted by a theory valid in the macroscopic dielectric formalism of the effects of surface roughness on the bulk modes. It is suggested that surface roughness introduces new boundary conditions for the Maxwell equations so that the surface modes have some radiative character. For an unroughened crystal surface, a frustrated total reflectance experiment could detect surface excitons and an attempt to do this is described. These experiments lead to a clearer understanding of the role of the surface in determining the optical and other properties of crystal anthracene.

INTRODUCTION

The role which a surface of a molecular crystal plays in determining observed electronic properties of the crystal is little understood. The paucity of experimental techniques for a study of optical phenomena associated with surface excitons and the difficulty in developing adequate theoretical understanding of such states on a real crystal surface contribute to this problem. While it is recognized that the nature of the surface as an imperfect interface permits a number of localized states associated with defects, adsorbed molecules, etc., the occurrence and form of surface bands—delocalized states—is a question of some importance in view of the many processes which involve either events sub-

sequent to the migration to the surface of excitons formed in the bulk or consequent upon surface exciton production. In recent years surface excitations (both plasmons and phonons) have been used as a diagnostic tool for characterizing the surfaces properties of metals and other materials.[1] It is possible that surface excitons may perform a similar role in molecular crystals.

Within an isotropic semi-infinite crystal of isotropic molecules when retardation is neglected and only nearest neighbour interactions are considered, the normal modes are separable into two types – surface and bulk[2] when there are no changes in the short range forces for molecules on the surface. The surface modes decay exponentially from the surface while the bulk modes have an oscillatory spatial dependence. Outside the crystal the same distinction can be made – both radiative modes (oscillatory dependence) and non-radiative modes (exponentially damped) exist. Therefore four types of normal mode exist when all the combinations are considered but photons which have an oscillatory spatial dependence couple only with the radiative modes. Non-radiative surface phonons[3,4] and surface plasmons[5] have been detected but there is no experimental evidence for the excitation of surface excitons which arise in this way. However, two types of surface excitons may exist. Firstly, for a crystal in which near-neighbour interactions are dominant, non-radiative surface excitations may arise from the long-range Coulomb forces assuming that all molecules experience the same short-range forces. Such a situation has been studied for phonons[2,6] and for excitons.[7] In this approximation the dielectric formalism is valid and surface modes exist which decay exponentially into the crystal as e^{-r/r_0} where r_0 is much larger than a lattice parameter. Secondly, radiative surface excitations may arise from the change in the short-range forces experienced by molecules at the crystal surface. Sugarkov's criterion[8] for their excitation is that the change in energy of the surface molecules due to alteration of the short-range forces should exceed the electronic bandwidth arising from dipole dispersion. It is expected[9] that this criterion is obeyed in the crystal system discussed here.

The long-range (macroscopic) forces dominate[10,11] the properties of the first electronic transition of crystal anthracene so the first type of surface exciton should be excited. Its presence is dependent on the orientation of the surface with respect to the principal axes of the dielectric permittivity tensor, the values of the principal components of that tensor and the non-analytic behaviour of the intermolecular interactions.

The observation of surface modes might be achieved by

i) Emission studies. Surface plasmon emission was observed[12,13] when metal foils were bombarded by an electron beam at oblique incidence. However, emission is not expected from surface excitions because the relaxation processes may be expected to be as fast as those for bulk excitons and any surface excitons may be rapidly scattered into the bulk exciton density-of-states. Also extremely

fast charge-pair generation may occur as well as any other non-radiative decay paths which occur at a crystal surface.

ii) Reflection spectra from non-planar interfaces. Surface plasmons in Al and Ag are manifested by dips[14] in the reflection spectra from thin cylinders ($\sim$ 50 μ diameter). In such a geometry some of the surface modes become radiative and interact with light. Molecular crystals which crystallize as long, thin needles would be ideal for such an experiment although the anisotropic nature of the dipole forces would cause interesting effects.

iii) The normal incidence reflectance spectra of roughened surfaces. Both random[15,16] or regular[17,18] (e.g. ruled grating) surface roughness will produce such effects.

iv) Frustrated total reflection (FTR) experiments have shown the existence of both surface phonons[3,4,19] and surface plasmons[5,20]. Evanescent light which may couple directly with the non-radiative crystal modes is produced by a refractive material such as silica separated from the crystal by a small distance. Provided that these modes are not totally destroyed by the surface roughness, it is expected that surface excitons in molecular crystals may be excited under the correct conditions.

There has been a report of the observation of radiative surface excitons[21] in crystal anthracene probed on the (ab) face, but the same spectral observations have been attributed[22] to resonances arising both from strain induced by lattice contraction upon cooling and from other crystal defects which may or may not be localized near the surface. From one viewpoint anthracene is a suitable choice of a molecular crystal to probe for the presence of surface excitons because of the detailed knowledge[10,11,23] of the dielectric permittivity tensor and because of existing calculations of surface states[8,24] and thin crystal effects[7,25] in anthracene. Unfortunately, theoretical development of surface waves (plasmons, phonons, excitons) appears to have reached only a treatment of a uniaxial crystal of isotropic molecules.[19] A biaxial crystal of anisotropic molecules such as anthracene is a very difficult problem indeed and lack of adequate theory by which to treat experimental data could limit analysis of such data.

However, despite these problems we present evidence in this paper for the existence of surface roughness induced excitation of surface excitons. An attempt to use the FTR method to excite surface excitons is described and the results lead to a clearer understanding of the conditions needed for their observation in molecular crystals.

EXPERIMENTAL AND RESULTS

Reflection spectra were taken using a reflection spectrometer described elsewhere[23,26].

Surface roughness experiments

A solution-grown anthracene crystal was cleaved along the (ab) face. One half of the crystal surface was left physically unperturbed while the other half was roughened slightly using a very fine emery paper. The surface took on a white appearance because of light scattering from small crystallites strewn on the surface. These were removed by lightly polishing with a xylene-soaked tissue paper. The crystal regained its transparent nature but this surface was dull compared with the physically unperturbed surface. The crystal was glued with GE 7031 adhesive on the copper block of a cryostat using a one-point mounting technique and with the b axis horizontal. A well collimated polarized light beam (1 mm^2 on the crystal) with an angle of convergence of 3° in the (ac) plane and 10′ in the (bc′) plane was translated horizontally across the crystal surface (8 mm wide) by a rotating silica block. A reference silica prism was placed beside the crystal. The reflected light was deflected by a 45° partially aluminized mirror and collected by a single photomultiplier.

The time-shared photomultiplier signal consisted of three regions—unperturbed crystal I_o, perturbed crystal I_p, and the silica reference I_M. Portions of the signal were gated and the ratios I_p/I_o, I_p/I_M, and I_o/I_M calculated electronically using a ratiometer which has an accuracy of 1% over a dynamic range of 4 decades. These ratios were recorded on strip chart recorders as a function of wavelength.

In Figs. 1, 2 are shown the low temperature reflectance (I_o/I_M) spectra from the unperturbed crystal surface. A b-polarized spectrum ($I_p(\omega)/I_o(\omega)$) taken at 296°K, before cool down, is shown in Fig. 3 as well as the spectrum after

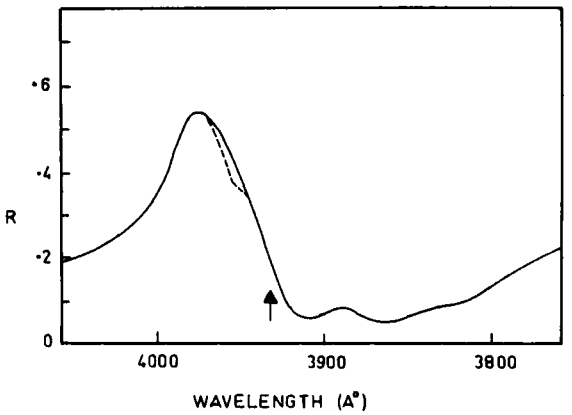

FIGURE 1 The b polarized normal incidence reflection spectrum from the (ab) face of anthracene crystal (from the unperturbed surface) at 80°K 10 minutes (– – – –) and 7 hours(———) after cooldown.

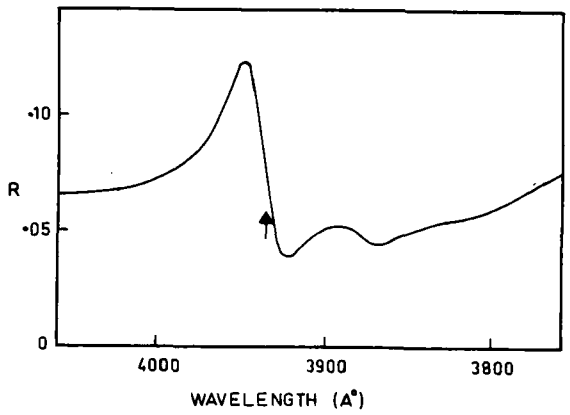

FIGURE 2 The a polarized normal incidence reflection spectrum from the (ab) face of anthracene crystal (from the unperturbed surface) at 80°K. The spectrum did not alter with time.

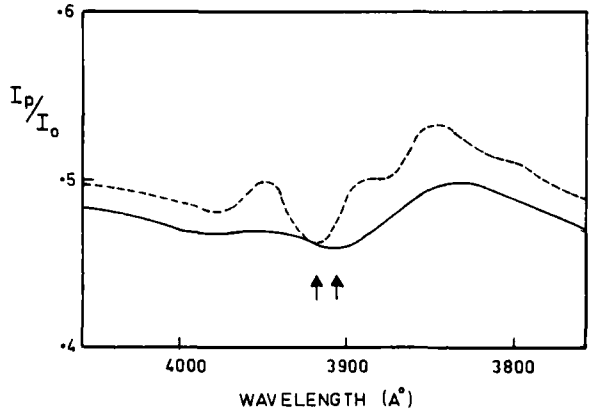

FIGURE 3 The b polarized spectrum I_p/I_0 for light normally incident on the (ab) face of an anthracene crystal. I_p is the reflected intensity from a roughened surface while I_0 is that from a freshly cleaved crystal. Temperatures were 296°K (———) and 155°K (– – – – –). The surface exciton resonance frequencies are indicated by arrows. (Arrow at higher wavelength for 155°K data.)

cooling the crystal to 155°K in 50 minutes. Further cooling of the crystal to 80°K in 30 minutes produced the spectra of Fig. 4.

Surface coupling experiments

Thin sublimation flakes (about 20 μ thick) were grown from ultra-purified anthracene. The developed (**ab**) face was placed on the hypotenuse side of an

optically polished silica prism. Portions of the crystal adhered optically to the prism and in other regions small air gaps were present. Optical interference patterns could be observed from these regions as the prism was rotated towards the critical angle, and the spatial separation of the observed fringes showed that a range of air thicknesses was produced.

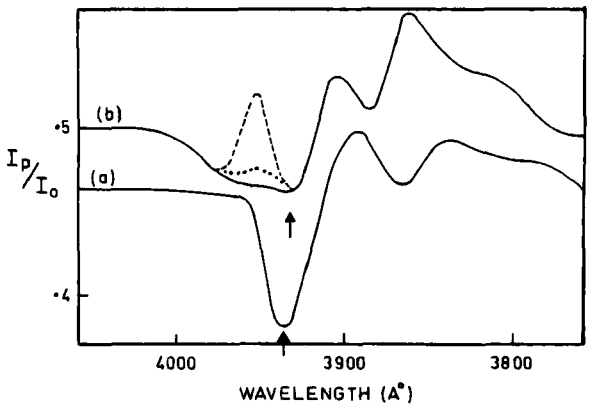

FIGURE 4 The a and b polarized spectra I_p/I_0 for light normally incident on the (ab) face of an anthracene crystal at 80°K. The surface exciton resonance frequencies are indicated by arrows. The b polarized spectra are taken (after 80°K was established) at 10 minutes (– – – – –), 3 hours (. . .) and 7 hours (———).

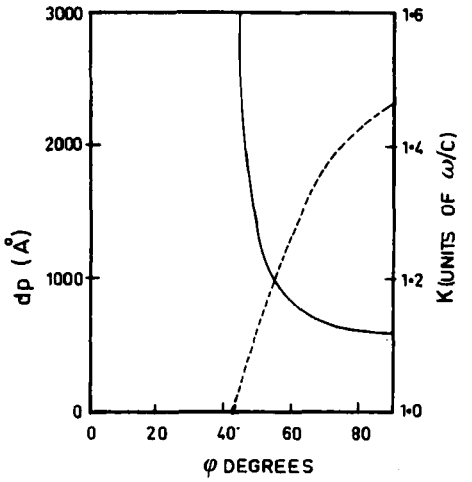

FIGURE 5 The depth of penetration (dp) and component of the wavevector along the surface (k) of the evanescent light produced by a prism of refractive index 1.469 as a function of the angle of incidence (ϕ) at a silica-air interface.

The crystal was oriented so that the b axis was parallel to the basal triangular plane of the prism and P-polarized light (electric field in the plane of incidence) propagated in the (bc') plane. When the prism is rotated past the silica-air critical angle a beam of exponentially damped (evanescent) light is produced which penetrates the air gaps to a depth d_p, shown in Fig. 5 for a wavelength of 4000 Å. This depth is calculated from the relationship[27]

$$d_p = \frac{0.693\,\lambda}{4\pi(n_0^2 \sin^2\phi - 1)^{\frac{1}{2}}} \tag{1}$$

where n_0 is the refractive index of silica (=1.469). This evanescent light which is characterized by a complex angle of refraction, a wavevector parallel to the prism surface and electric field in the plane of incidence should interact with the exponentially damped (non-radiative) crystal modes, creating a dip in the reflectance at the resonance frequency of these modes.

Spectra were taken at various angles of incidence past the critical angle at temperatures of 296°K and 77°K and for a range of air gap thicknesses. No evidence for the non-radiative crystal modes was obtained.

DISCUSSION

Surface roughness spectra—Spectral analysis

It should first be made clear that the spectrum from the perturbed area $I_p(\omega)$ differs from that from the unperturbed area $I_0(\omega)$ only by (i) a reduction in the specular reflectance intensity due to incoherent scattering, (ii) an alteration in shape on the high energy side of the band which is sharply reflected in the ratio spectrum $I_0(\omega)/I_p(\omega)$—a sensitive monitor of a band shape alteration especially when each component is varying over a wide range. $I_p(\omega)$ still retains the main polarization characteristics of $I_0(\omega)$ suggesting together with observations (i) and (ii) above that the surface treatment did not grossly disturb the optical properties.

From the spectra in Fig. 1 it is seen that there is a time dependence of the b-polarized spectrum in the region near 3953 Å. The reflectance dip which disappears with time observed there has been related[22] to the effect of crystal strain. Cooling produces plastic deformations in thick crystals which, being mobile when single point mounting is employed, anneal out with time. The spectral feature can be explained as a resonance which arises from lattice dilation around the dislocation. At the same frequency, a peak is observed in the ratio $I_p(\omega)/I_0(\omega)$ (Figures 3, 4). It disappears with time (Figure 4) and is probably associated with the same dislocation effect.

Observation of this I_p/I_o peak implies that the dislocations anneal out more rapidly in the roughened than the unroughened crystal. Because the crystal is strongly absorbing in the region of 3953 Å, the dislocations probed must lie close to the surface and a distinction between surface roughness and the internal roughness probed by the light becomes unclear. However, the peak anneals out with time and the motion of dislocations–which implies the motion of molecules–is made easier near a roughened surface. The spectrum at 155°K, which was taken immediately after cooldown, (Fig. 3) also shows this peak.

The dips in the ratio spectrum $I_p(\omega)/I_o(\omega)$ which do not alter with time are correlated with the maxima in the reflectance spectrum, but shifted to higher energy so that they appear at energies just below the reflectivity minima. In Figures 3 and 4 the dips in $I_p(\omega)/I_o(\omega)$ for the 0-0 band are indicated by arrows. These dips also appear for each resolved vibronic state and the depth of the dip is largest for the strongest vibronic transitions.

The frequencies of the dips for the 0-0 transition are given in Table 1, in which, in anticipation, the dip frequency is associated with the surface excition resonance frequency.

Surface roughness spectra—Theoretical analysis

Surface roughness leads to both incoherent and coherent scattering. The normal incidence specular reflection $R(\omega)$ from a rough surface of an isotropic crystal of isotropic molecules when incoherent scattering occurs is given by[28]

$$R(\omega) = R_o(\omega)\, e^{-(4\pi\sigma/\lambda)^2} \tag{2}$$

for a Gaussian distribution of irregularities, where $R_o(\omega)$ is the reflectance from a perfectly smooth surface and σ is the r.m.s. roughness which may be equated

TABLE I

Surface exciton resonance frequencies of the anthracene 0-0 crystal transition measured as experimental frequencies of dips in the ratio $[I_p(\omega)/I_o(\omega)]$ spectrum of crystal anthracene probed on the (ab) face, and the frequencies of the minimum of $|\epsilon(\omega)+1|$ deduced from $I_o(\omega)$ data (I_p, I_o intensity of light reflected from a perturbed and unperturbed surface respectively, ϵ the dielectric permittivity.)

Temperature (°K)	Polarization of Incident Light	Frequency (cm^{-1}) I_p/I_o	$\lvert\epsilon(\omega)+1\rvert_{MIN}$
296	b	25600 ± 10	25615 ± 12
155	b	25520 ± 10	25530 ± 12
80	b	25420 ± 10	25455 ± 12
80	ac	25405 ± 10	25435 ± 12

to the r.m.s. height of the surface bumps. Incoherent scattering is caused by the phase fluctuations in path length of rays striking different parts of the crystal surface.

However, the photomultiplier collects not only the specular reflection but also some of the diffuse reflection, and the detected reflectance, under the same assumptions as Eqn. 2, is of the form[29]

$$R(\omega) = R_0(\omega)\left[e^{-(4\pi\sigma/\lambda)^2} + \frac{2^5\pi^4}{m^2}\left(\frac{\sigma}{\lambda}\right)^4 (\Delta\theta)^2\right] \tag{3}$$

where m is the r.m.s. slope of the surface profile and $\Delta\theta$ is the (solid) acceptance angle of the collection optics. For the optical system used $\Delta\theta = 0.008$ ster. and only values of $m \approx 1/100$ would make a significant contribution. By a comparison of the measured reflectance at 4200 Å with that predicted from refractive index data, it is estimated that $\sigma \leq 90$ Å for the unperturbed surface of the crystal used. The frequency dependence of equation (3) is weak—the specular component decreases while the diffuse component increases as the energy increases. Therefore incoherent scattering alone cannot account for the results unless the equivalent of Eqn. 3 for a biaxial crystal of anisotropic molecules has a marked frequencey dependence.

An estimate of the extent of the surface roughness induced by the artificial roughening can be made. Since the measured value of $I_p(\omega)/I_o(\omega)$ (b-polarization) is approximately 0.5 at lower frequencies than the absorption region the value of σ for the roughened area may be calculated from Eqn. 2 as about 260 Å using the value of σ for the unroughened area as 90 Å. Hence, the roughening procedure, followed by crystal polishing, does not grossly disturb the crystal surface.

If incoherent scattering does not account for the results, will coherent scattering of radiation by surface roughness be important? This has been well studied in metals[30] where the surface plasmon from surface roughness induced excitation[18] is detected by a dip in the reflection spectrum at some frequency.

To understand the effects of coherent scatering, we use a classical theory of Berreman[31] which expresses the normal incidence reflectance $R(\omega)$ from a rough surface characterized by N bumps or pits per unit area with an average volume V as

$$R(\omega) = R_0(\omega)\left(1 - \frac{NV\partial[\epsilon(\omega)]}{\lambda}\right) \tag{4}$$

where $\partial[\epsilon(\omega)]$ is a form factor which depends on the dielectric permittivity, presumed to be that for an isotropic solid of isotropic molecules and to a limited extent on the shape of the irregularity. If diffuse scattering is included, then $R_0(\omega)$ is replaced by $R(\omega)$ of equation (3). Thus the ratio $I_p(\omega)/I_o(\omega)$ of Figures 3 and 4 may be regarded as being proportional to the function

$$\frac{1 - (NV)_p \lambda^{-1} \partial\{\epsilon(\omega)\}}{1 - (NV)_0 \lambda^{-1} \partial\{\epsilon(\omega)\}}$$

where $(NV)_p$ and $(NV)_0$ are the average heights of bumps on the roughened and unperturbed surface respectively. If, as expected $(NV)_p \gg (NV)_0$, then

$$\frac{I_p(\omega)}{I_0(\omega)} \propto 1 - (NV)_p \lambda^{-1} \partial[\epsilon(\omega)] \tag{5}$$

The effective dielectric permittivity $\epsilon(\omega)$ $[= \epsilon_1(\omega) + i\epsilon_2(\omega)]$ for $k \perp (ab)$ for both polarization directions was calculated from the normal incidence unperturbed spectrum using a fast Fourier transform technique.[32] These results are shown in Figure 6. Using the data from the b polarized spectra, the spectrum of $\partial\{\epsilon(\omega)\}$ was calculated using an irregularity shape which has been described elsewhere[9,33]. This spectrum is shown in Figure 7 for b polarized light. The frequency at which ∂ is a maximum is relatively insensitive to the irregularity shape but quite dependent on ϵ_1 and ϵ_2. Note from Fig. 7 that a maximum in $\partial\{\epsilon(\omega)\}$ is observed at 25420 cm^{-1} ($\epsilon_1 = -0.18$, $\epsilon_2 = 1.7$) which coincides with the experimental value (see Table 1) of the resonances ascribed to the roughness induced surface exciton.

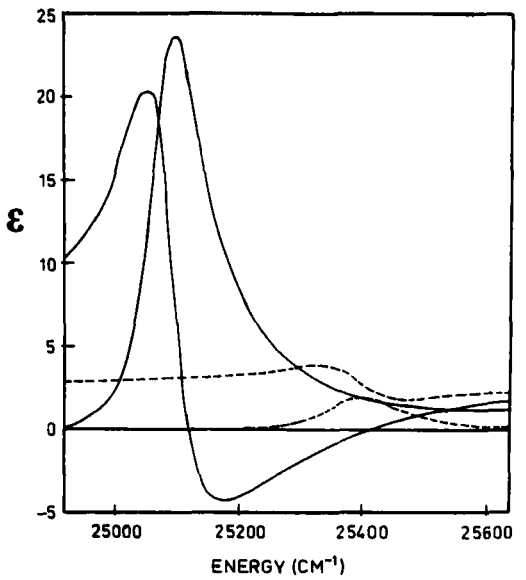

FIGURE 6 The real and imaginary parts of the dielectric permittivity $\epsilon(\omega)$ for b polarized (——) and a polarized (– – – –) light normally incident on the (ab) face of crystalline anthracene at 80°K.

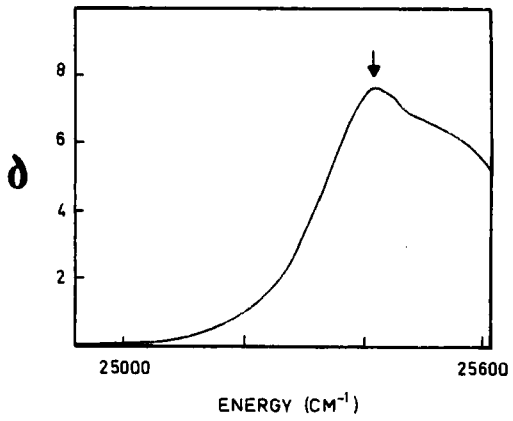

FIGURE 7 Spectrum of the form factor ∂ calculated from the b polarized $\epsilon(\omega)$ data at 80°K (see Figure 6) using a theory valid in the macroscopic dielectric formalism.

From the maximum value of $\partial(=7.6)$ an upper limit to $(NV)_p$ is 280 Å assuming that the total loss is due to coherent scattering. Outside the absorption region where the coherent scattering is negligible, there is substantial diffuse scattering which should decrease the value of NV. However, it is worth noting that (i) The estimate of the r.m.s. surface roughness of the perturbed surface, $\sigma = 260$ Å, is very similar to the value of $(NV)_p$ deduced in the above calculation. It is expected that σ would provide an upper limit of $(NV)_p$. (ii) The occurrence of a minimum in $I_p(\omega)/I_o(\omega)$ when $\partial\ \epsilon(\omega)$ is a maximum is consistent with Eqn. 5 and illustrates the effects of surface roughness.

A rough surface introduces new boundary conditions into the solution of Maxwell's equations so that the new surface modes in a roughened crystal have some radiative character. From analogy with the evidence for a surface plasmon [18,30], we suggest that the experimental results of Table 1 provide the resonance frequencies at different temperatures of the surface roughness induced surface excitons.

Is it possible to decide which type of surface excitons, if indeed they are distinct in a surface roughened crystal, is being observed in this experiment? It is known from experiment[19] and theory [34,35] that the properties of surface excitons in anisotropic crystals are quite complex even in the case of no non-analytic behaviour of the macroscopic fields. For example, if the surface contains the optic axis of a uniaxial crystal, then ordinary surface excitons are excited when the direction of propagation in the surface is perpendicular to this axis. This is of pure transverse character and is similar to a surface exciton in an isotropic media. The surface excition resonance condition is $\epsilon_\perp = -1$ when damping is not considered. However, for propagation parallel to the optic axis

extraordinary surface excitons may propagate. These modes are of mixed transverse-longitudinal character and possess a resonance condition $\epsilon_{\parallel}\epsilon_{\perp} = 1$ when damping is neglected. If both $\epsilon_{\parallel}$ and $\epsilon_{\perp}$ are negative then the extraorinary surface excitons are real, whereas if the dielectric permittivity perpendicular to the direction of propagation (ϵ_s) is positive then these surface modes propagate only when $\epsilon_s > 1$. In the case where $0 < \epsilon_s < 1$, no real modes propagate but "virtual excitation" surface excitons do exist.[19] These have a real disperson only over a limited region of propagation vector **k**. Biaxial crystals are even more complicated and no treatment of surface excitons in biaxial crystals with non-analytic behaviour of the macroscopic fields exists. So it is unsure to which if any of these types of surface excitons that observed in the surface roughness experiment corresponds.

As mentioned above, surface excitons propagate in an isotropic crystal of isotropic molecules if damping is neglected when $\epsilon_1 = -1$. When damping is considered, this condition is modified to $|\epsilon(\omega) + 1|_{MIN}$. using a macroscopic dielectric approach. In Table 1, the frequencies at which $|\epsilon(\omega) + 1|$ is a minimum are given. The agreement with the values at which we suggest surface roughness induced surface excitons propagate are excellent. Why does the simple condition $|\epsilon(\omega) + 1|_{MIN}$ predict the energy of the roughness induced surface exciton for both polarizations? This condition is true for isotropic crystals and uniaxial crystals for propagation directions normal to the optic axis when that axis lies in the surface. However for other directions the situation is more complex. For example, with extraordinary surface excitons, in uniaxial crystals the condition is $\epsilon_{\perp}\epsilon_{\parallel} = 1$ when damping is not considered. For the case of the 0-0 transition of anthracene, the frequency of the $\mathbf{k} = 0$ longitudinal exciton (when $\epsilon_1(\omega)$ has a minimum value when damping is included[36]) is nearly independent of the polarization vector when light is normally incident on the (**ab**) face. Neglecting damping, it is possible that the condition $\epsilon = -1$ then occurs at similar frequencies for both polarization directions, since the surface exciton frequencies lie only slightly below the longitudinal exciton frequencies. Therefore, any condition of the type $\epsilon_{\perp}\epsilon_{\parallel} = -1$ will occur when both $\epsilon_{\perp} = -1$ and $\epsilon_{\parallel} = -1$. These are the conditions for an isotropic crystal. Hence, the near-degeneracy of the longitudinal excitons for this transition may simplify the dielectric conditions such that the resonance frequencies of the surface excitons are predicted from the isotropic crystal condition.

The F.T.R. experiment

Why did not the FTR experiment give evidence of these surface excitons? In virtue of the novelty of this experiment for molecular crystals it is useful to consider this point briefly. Firstly, the problems of the experimental performance of the experiment are discussed, then the effects on the results of the wavevector

dependence of the dielectric permittivity are considered using two simple models and finally the effects that the surface roughness on real molecular crystals have on the expected results are calculated.

The experimental conditions

The sensitivity of the measuring technique was such that a change of 0.25% in R would have been detectable. As shown in Fig. 5, the air gap, d, is an important parameter. Whilst this varied from one crystal to another, the regularly spaced interference pattern observed by rotating the crystal-air-silica interfaces past the critical angle did indicate a uniform spacing over an area large compared with the probe beam size. In general, the probe area was about 30% of the crystal area over the air gap. The air gap thickness could not be measured accurately. However, it seems that with the large range of thicknesses used and the sensitivity of the detection system some evidence of a resonance should have been seen.

A model of an isotropic crystal of isotropic molecules

For this model, the optical properties may be described by the scalar dielectric permittivity $\epsilon(\omega)$ which is independent of the wavevector **k** provided that the effects of spatial disperson can be neglected. It can be inferred from experiment[11] and theory[9] that spatial dispersion (the **k** dependence of $\epsilon(\omega)$) causes negligible effects related to the magnitude of the wavevector $|\mathbf{k}|$. However, effects from the direction dependence of the wavevector, $\hat{\mathbf{k}}$, which arise from molecular anisotropy, are important and are considered in the next section. Neglecting spatial dispersion, the dielectric permittivity $\epsilon(\omega)$ corresponds to that measured at normal incidence (data of Fig. 6). If the model were suitable, the a and b polarized spectra would be identical.

The reflected light in the FTR experiment using p-polarized light is given by[37]

$$R(\omega) = |r(\omega)|^2 \tag{6a}$$

$$r(\omega) = \frac{r_1 + r_2(\omega)\, e^{2i\beta(\omega)}}{1 + r_1 r_2(\omega)\, e^{2i\beta(\omega)}} \tag{6b}$$

$$\beta(\omega) = \frac{2\pi}{\lambda} n_1 d\, a_1 \tag{6c}$$

$$r_1 = \frac{n_0 a_1 - n_1 \cos\phi}{n_0 a_1 + n_1 \cos\phi} \tag{6d}$$

$$r_2(\omega) = \frac{n_1 a_2(\omega) - n_2(\omega) a_1}{n_1 a_2(\omega) + n_2(\omega) a_1} \tag{6e}$$

$$a_1 = \left[1 - \left(\frac{n_0 \sin\phi}{n_1}\right)^2\right]^{\frac{1}{2}} \tag{6f}$$

$$a_2 = \left[1 - \left(\frac{n_0 \sin\phi}{n_2(\omega)}\right)^2\right]^{\frac{1}{2}} \tag{6g}$$

where $n_2(\omega) = \epsilon(\omega)^{\frac{1}{2}}$, $n_1 = 1$, $n_0 = 1.469$, d = the air gap thickness and ϕ the angle of incidence at the silica-air interface. The spectrum of $R(\omega)$ is shown in Fig. 8 using the b polarized data of Fig. 6 and d = 1000 Å. As can be seen, this model predicts a large series of dips of a magnitude that should be readily observed experimentally.

A model of an isotropic crystal of anisotropic molecules

Although anthracene is a monoclinic crystal this model leads to[11] computed oblique angle reflectance spectra in good agreement with experimental spectra. Using this model, the a and b polarized normal incidence spectra are different and the resonance frequencey, which probes the exciton band structure, is a function of the direction of propagation $\hat{\mathbf{k}}$. For a model calculation of the expected FTR results based on this simple concept of the crystal, we proceed as follows. The dielectric permittivity, $\epsilon(\hat{\mathbf{k}},\omega)$ is given[11] by

$$\epsilon(\hat{\mathbf{k}}, \omega) = \epsilon \left[\frac{\omega^2 - \omega_z^{(1)}(\hat{\mathbf{k}})^2}{\omega^2 - \omega_p^{(1)}(\hat{\mathbf{k}})^2}\right] \left[\frac{\omega^2 - \omega_z^{(2)}(\hat{\mathbf{k}})^2}{\omega^2 - \omega_p^{(2)}(\hat{\mathbf{k}})^2}\right] \tag{7}$$

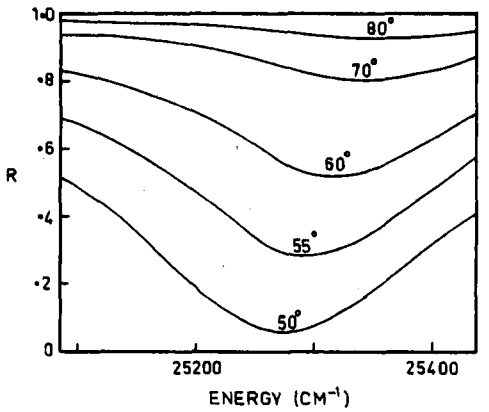

FIGURE 8 The FTR spectra computed using the b polarized $\epsilon(\omega)$ data of Fig. 6 expected for different angles of incidence and with an air gap of 1000 Å. A spectrum would be observed on the (ac') crystal face.

where $\omega_p^{(1)}$, $\omega_p^{(2)}$ are the poles and $\omega_z^{(1)}$, $\omega_z^{(2)}$ the zeros which map the exciton band structure around $\mathbf{k} \approx 0$ as a function of $\hat{\mathbf{k}}$. Equations for ω_z and ω_p, which are complicated even under the approximations used, are given in Ref. 11. Using $\epsilon_0 = 3.0$, the oscillator strength $f_1 = 0.0356$, the crystal-shifted molecular resonance frequency as 25900 cm^{-1} and the dipole sums of Philpott[38], the poles and zeros were calculated. The results are shown in Fig. 9. Now η measures the angle between the normal to the (ab) plane and the direction of propagation. In the surface coupling experiment $\eta = 90°$ since the direction of propagation is along the surface. Since the light is polarized in the (bc′) plane, the experimental situation is described in Fig. 9 by R_p(bc′) at $\eta = 90°$. In this case $\omega_p^{(2)} \equiv \omega_z^{(1)}$ and the blocking band width is given by $\omega_z^{(2)} - \omega_p^{(1)}$. This width is a measure of the oscillator strength. Note that the width is equivalent to that measured by $\omega_z^{(2)} - \omega_p^{(2)}$ for R_s(ac) at η=0 in Figure 9, and $\omega_p^{(2)}$ (η=0, R_s(ac)) $\equiv \omega_z^{(2)}$ ($\eta = 90°$, R_p(bc)). That is, the spectrum observed for a polarized light normally incident on the (ab′) face is equivalent to that measured for c′ polarized light normally incident on the (ac′) face except that the latter is shifted to lower energy by $\omega_z^{(2)} - \omega_p^{(2)}$ as measured from the former. In Figure 6, ω_p is measured at the maximum of $\epsilon_2(\omega)$, and ω_z at the minimum of $\epsilon_1(\omega)$, so that

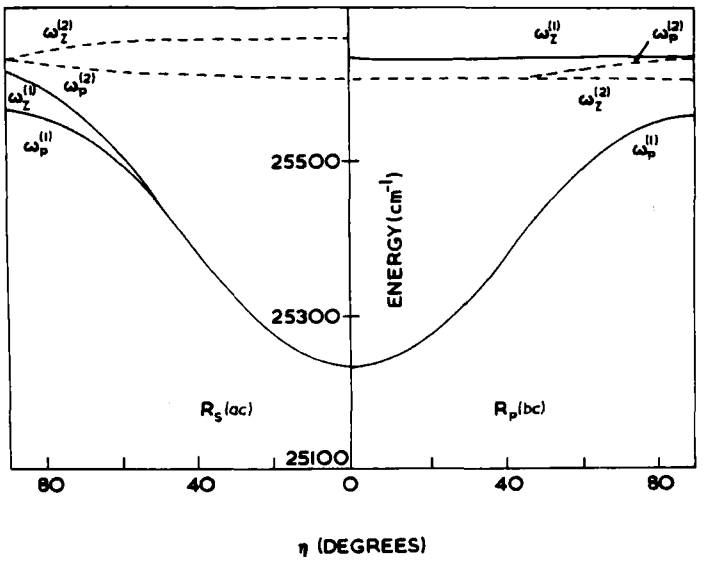

FIGURE 9 The exciton band structure of crystal anthracene about $\mathbf{k} = 0$ calculated using a dipole theory. The angle η is measured between the normal to the (ab) face and the direction of the propagation vector k. The graph gives the variation of the frequencies of the poles and zeros with η for the polarization vector in the (bc′) plane for $\mathbf{k} \parallel$ (bc′) {R_p (bc′)} and for the polarization vector $\hat{e} \parallel a$ for $\mathbf{k} \perp a$ {R_S (ac)}.

$\omega_z - \omega_p \approx 60\ cm^{-1}$ Therefore, shifting the a polarized spectrum in Fig. 6 downfield by 60 cm^{-1} the dielectric permittivity for k ∥ (ab) is obtained within the approximations used. Substituting these results into equations (6) the FTR spectrum is calculated for d = 1000Å and various angles of incidence. The results are shown in Figure 10.

Note from Figures 8 and 10.

i) The minimum of $R(\omega)$ shifts to higher energies with increasing angle of incidence. The surface exciton frequency measured at this minimum is a function of the magnitude of the wavevector along the surface, $k(\omega)$ $(= \omega/c\ n_o \sin\phi)$ which is plotted in Fig. 5. The surface exciton dispersion relationship is given by

$$k(\omega) = \frac{\omega}{c}\left|\frac{\epsilon_1(\omega)}{\epsilon_1(\omega)+1}\right|^{\frac{1}{2}} \tag{8}$$

for $\epsilon_1 < 1$. This is plotted in Figure 11 for the b polarized dielectric permittivity. For the a polarized data, ϵ_1 is always positive, so $k(\omega)$ cannot be defined. Note, as discussed earlier that Eqn. 8 is valid only for cubic and special cases of uniaxial crystals, but the data of Fig. 11 illustrates the dispersion of the surface exciton in this simple model. For a more realistic model of a biaxial crystal both the dispersion and the reasonance condition excluding damping from Eqn. 8 $(\epsilon_1(\omega) = -1)$ would be altered although the latter perhaps not markedly as discussed earlier, However, the dispersion would depend on the type of surface excition.

ii) The half-widths of $R(\omega)$ in Figures 8 and 10 decrease with increasing angle of incidence. This half-width has two components; one (independent of ϕ) due to the internal relaxation processes, predominantly exciton-phonon scattering, and

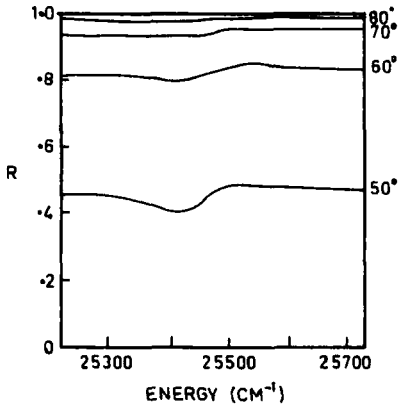

FIGURE 10 The FTR spectra computed using the a polarized $\epsilon(\omega)$ data of Fig. 6 expected for different angles of incidence and with an air gap of 1000 Å. A spectrum would be observed on the (ab) crystal face.

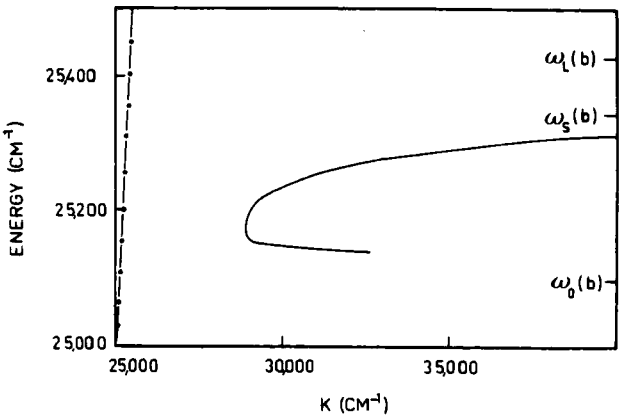

FIGURE 11 The dispersion of the surface exciton (———) calculated as a function of the wavevector (k) using the b polarized data of Fig. 6. The dispersion of light propagating in a vacuum (–·–·–·) is also shown. The frequencies $\omega_0(b)$, $\omega_S(b)$ and $\omega_L(b)$ represent the transverse bulk exciton, surface exciton, and longitudinal bulk exciton resonance frequencies.

the other arising from the finite radiative damping. The latter is proportional to $e^{-(\omega d/c)(n_0^2 \sin^2\phi - 1)}$ and is larger at the lower angles. As d becomes infinite, the radiative contribution vanishes implying that in the FTR experiment the surface modes become partly radiative in character.

Effect of the surface roughness on the FTR results

It was earlier argued that some surface roughness gives some radiative character to the surface modes, In this section, the effect of the surface roughness on the FTR spectrum is calculated from the ϵ data of Figure 6 using Berreman's theory [31], and Eqn. 6 in the limit NV $\ll$ d where the term $r_2(\omega)$ measures the amplitude of the reflectance from the crystal when the cosine of the angle of incidence on the crystal (a_1) is complex as in the FTR experiment. This approach assumes that the surfaces used in the normal incidence experiment were completely smooth while those of the FTR experiment were rough. This is not true but only qualitative arguments are valid here because the model used, an isotropic crystal with isotropic molecules, is not expected to give a complete analysis.

The effect of surface roughness is severe and some results are shown in Fig. 12 (b-polarized data) and Fig. 13 (a-polarized data) at 50° angle of incidence at the silica-air interface for d = 1000 Å. At large NV (e.g. 150 Å) two resonances are seen. One is a new dip in the vicinity of the peak of $\epsilon_2(\omega)$. This occurs because crystal surface roughness induces non-radiative character into modes which are radiative for a perfect surface. Predictably this reflectance dip increases with increased surface roughness. At low values of NV (e.g. 25 Å) this

effect causes a distortion which can shift the reflectivity minimum arising from the surface exciton resonance to slightly lower energies. At large values of NV, the surface exciton resonance is shifted to higher energies and the spectral distortion is very large.

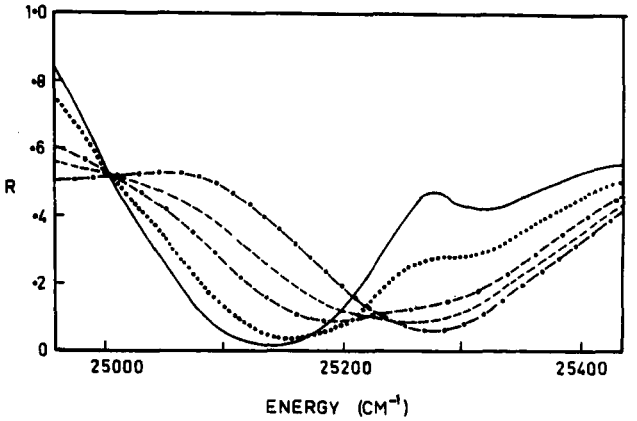

FIGURE 12 The effect of surface roughness (NV) on the FTR spectrum of Fig. 8 at $\phi = 50°$ calculated as indicated in the text for the following values of NV.

—·—·—	NV = 0	(smooth surface)
– – – –	25 Å	
– – · – – ·	50 Å	
·····	100 Å	
———	150 Å	

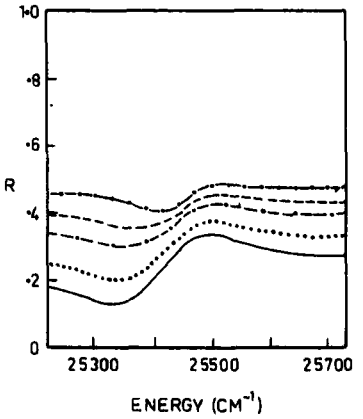

FIGURE 13 The effect of surface roughness (NV) on the FTR spectrum of Fig. 10 at $\phi = 50°$ calculated as indicated in the text for the following values of NV.

—·—·—	NV = 0	(smooth surface)
– – – –	25 Å	
– – · – – ·	50 Å	
·····	100 Å	
———	150 Å	

CONCLUSIONS

One of the major problems in studying surface excitons in a molecular crystal such as anthracene is that the crystal and molecular anisotropy complicate the prediction of the observables in an optical experiment. The simplified models which must be used may obscure the expectations in a real crystal system. Yet despite this problem, we have argued from the normal incidence reflection spectra of artificially roughened crystals at various temperatures that the data provides evidence for the existence of surface exciton resonances in molecular crystals. The frequencies at which they occur correspond with those predicted by a theory based on changes in the long-range (dipole) interactions arising from surface roughness. However, a more direct probe for those surface excitons using an FTR technique led to no positive results. Because the theoretical development of surface excitons is still an immature subject, it is difficult to assess quantitatively the reason for this. The most sophisticated model used viz. an isotropic crystal of anisotropic molecules, may be quite crude although there is good evidence[11] that it is reasonable for explaining oblique angle reflectance data. It may well be that the roughness which exists even on the best surfaced molecular crystals prepared by sublimation techniques may be so randomized in values of NV over the optical probe area that any resonance is too distorted to be clearly recognized.

Further experimental and theoretical work in this important area is needed before firmer conclusions are possible. Bearing in mind that the requirement for a strong surface exciton resonance is that a large component of a strong transition moment lies perpendicular to the surface considered, future experiments could look for surface exciton resonances in molecular crystals by using light incident on the (**ab**) face of a perylene crystal or even the (**ac'**) face [$c' \perp$ (**ab**)] of an anthracene crystal provided that face could be obtained suitably smooth. If the crystal surface topology could be obtained e.g. from a combination of surface holography and multiple beam interference or from electron microscopy on decorated surface replicas, a measure of the distribution of surface defects, dislocations, etc. might be used to provide a quantitative estimate of how these would affect both the bulk and surface modes. Use of two photon absorption techniques to reduce the contribution of the surface modes relative to the bulk modes is also desirable especially for a decision on the presence of the radiative surface modes which decay within a lattice parameter. A comparison of one-photon reflection data $R(\omega)$ with two photon absorption data will help to decide the surface contribution to $R(\omega)$.

Also, if theory could develop to the stage of predicting the resonance condition for surface exciton propagation in a perfect surfaced biaxial crystal of anisotropic molecules more reliable comparison with experiment could be made. Extension of that theory to look at the effects of surface roughness on both the

(formerly) radiative and non-radiative modes would then be possible.

Whilst the surface of a real molecular crystal can produce alterations of the bulk crystal properties, the appearance of a surface exciton resonance in roughened crystals, the overall similarly between the form of $I_p(\omega)$ and $I_o(\omega)$ for each polarization and the results of work[11] probing the exciton band structure around $k = 0$, do not support an earlier conjecture[39] that the width of the 0-0 band is determined by crystal surface effects. That conjecture was based on experimental absorption data of others, now known[26] to be incorrect.

Finally, it should be remembered that many important processes involve the migration to the surface of singlet excitons formed in the bulk of the crystal e.g. charge injection phenomena. Our results indicate that surface excitons may be directly populated in surface roughened crystals at the appropriate frequency and, being localized on the surface, may show different characteristics from the bulk excitons e.g. the quantum yield of fluorescence may drop in favour of charge carrier or triplet exciton production if such processes occur at the surface. These processes would necessarily occur rapidly ($< 10^{-13}$ sec) or the surface exciton would scatter into the bulk exciton density-of-states which, of course, encompasses the surface exciton frequency. But since many molecular crystals used for a variety of experiments have quite rough surfaces the existence of and effects from surface excitons in such systems should not be overlooked.

Acknowledgements

We thank the Australian Research Grants Committee for support and the Commonwealth Scientific and Industrial Research Organization for a Studentship to M.G.S. One of us (G.C.M.) acknowledges the hospitality of Sir George Porter and the Royal Institution and a Royal Society Nuffield Foundation Bursary during tenure of which this work was prepared for publication.

References

1. Proc. of the Conf. on *Surface Properties and Surface States of Electronic Materials,* University of Missouri-Rolla (1972), Ed., W. J. James, in *Surface Science*, **4**, 1-176 (1973).
2. R. Fuchs and K. L. Kliewer, *Phys. Rev.*, **140**, A, 2076 (1965).
3. N. Marschall and B. Fischer, *Phys. Rev. Lett.*, **28**, 811 (1972).
4. V. V. Bryksin, Yu. M. Gerbstein and D. N. Mirlin, *Phys. Stat. Sol.* (b), **51**, 901 (1972).
5. A. Otto, *Zeit, Fur Phys.*, **216**, 398 (1968).
6. K. L. Kliewer and R. Fuchs, *Phys. Rev.*, **144**, 495 (1966); **150**, 573 (1966).
7. D. P. Craig and L. A. Dissado, *Proc. Roy. Soc. A.* **332**, 419 (1973).
8. V. I. Sugarkov, *Sov. Phys.-Solid State*, **5**, 1959, 1607 (1964); **10**, 2363 (1969); **14**, 1711 (1973): *Ukr. Fiz. Zh.*, **15**, 2059 (1970).
9. G. C. Morris and M. G. Sceats, *J. Chem Phys.*, (in press).
10. L. B. Clark and M. R. Philpott, *J. Chem. Phys.*, **53**, 3790 (1970).
11. G. C. Morris and M. G. Sceats, *Chem. Phys.*, **1**, 259 (1973).
12. W. Steinmann, *Phys. Rev. Lett.*, **5**, 470 (1960).
13. R. W. Brown, P. Wessel and E. P. Trounson, *Phys. Rev. Lett.*, **5**, 472 (1960).
14. C. Miziumski, *Phys. Lett.*, **40A**, 187 (1972).

15. V. Burker and W. Steinmann, *Phys. Rev. Lett.*, **21**, 143 (1968).
16. E. Schnatterly and S. N. Jasperson, *Phys. Rev.*, **188**, 759 (1969).
17. Ye-Yungteng and E. A. Stern, *Phys. Rev. Lett.*, 19, 511 (1967).
18. N. Marschall, B. Fischer and H. J. Queisser, *Phys. Rev. Lett.*, **27**, 95 (1971).
19. H. J. Falge and A. Otto, *Phys. Stat. Sol.* (b), **56**, 523 (1973).
20. A. S. Barker, Jr., *Phys. Rev. Lett.*, **28**, 892 (1972).
21. M. S. Brodin, M. A. Dudinskii and S. V. Marisova, *Opt. Spectrosc.*, **31**, 401 (1971).
22. G. C. Morris and M. G. Sceats, *Chem. Phys.* **1**, 376 (1973).
23. G. C. Morris and M. G. Sceats, *Chem. Phys.*, (in press).
24. P S. Stern and M. E. Green, *J. Chem. Phys.*, **58**, 2507 (1973).
25. A. S. Davydov, *Theory of Molecular Excitons*, Plenum, (N.Y.), 1971.
26. G. C. Morris and M. G. Sceats, *Chem. Phys.*, 1, 120 (1973);
27. N. J. Harrick, *J. Opt. Soc. Am.*, **55**, 851 (1965).
28. H. Davies, *Proc. I.E.E.* (Lond.), **101**, 209 (1954).
29. H. E. Bennet and J. O. Porteus, *J. Opt. Soc. Am.*, **51**, 123 (1961).
30. A. Dande, A. Savary and S. Robin, *J. Opt. Soc. Am.*, **62**, 1 (1972); and other references therein.
31. D. W. Berreman, *Phys. Rev. B*, 1, 381 (1970): *Phys. Rev.*, **163**, 855 (1967): *J. Opt. Soc. Am.*, **60**, 499 (1970).
32. M. G. Sceats and G. C. Morris, *Phys. Stat. Sol.*, **14** (a), 643 (1972).
33. G. C. Morris, S. A. Rice, M. G. Sceats and A. E. Martin, *J. Chem Phys.* **55**, 5610 (1971).
34. V. N. Lyubimov and D. G. Sannikov, *Sov. Phys.-Solid State*, **14**, 574 (1972).
35. A. Hartstein, E. Burstein, J. J. Brion and R. F. Wallis, *Surface Science*, **34**, 81 (1973).
36. D. W. Berreman, *Phys. Rev.*, **130**, 2193 (1963).
37. O. S. Heavens, *Optical Properties of Thin Solid Films*, (Butterworths, London, 1955), pp. 46-96.
38. M. R. Philpott, *J. Chem. Phys.*, **50**, 5117 (1969).
39. S. A. Rice, G. C. Morris and W. L. Greer, *J. Chem. Phys.*, **52**, 4279 (1970).